



LAWRENCE
LIVERMORE
NATIONAL
LABORATORY

Soft x-ray spectrometer operation at the National Ignition Facility

J. Schein, E. Dewald, K. Campbell, R. Turner, F.
Weber, M. Rhodes, O. Landen, M. B. Schneider, D.
Lee, V. Tran, D. Pellinen

May 7, 2006

High Temperature Plasma Diagnostics
Williamsburg, VA, United States
May 7, 2006 through May 11, 2006

Disclaimer

This document was prepared as an account of work sponsored by an agency of the United States Government. Neither the United States Government nor the University of California nor any of their employees, makes any warranty, express or implied, or assumes any legal liability or responsibility for the accuracy, completeness, or usefulness of any information, apparatus, product, or process disclosed, or represents that its use would not infringe privately owned rights. Reference herein to any specific commercial product, process, or service by trade name, trademark, manufacturer, or otherwise, does not necessarily constitute or imply its endorsement, recommendation, or favoring by the United States Government or the University of California. The views and opinions of authors expressed herein do not necessarily state or reflect those of the United States Government or the University of California, and shall not be used for advertising or product endorsement purposes.

Soft x-ray spectrometer operation at the National Ignition Facility

J. Schein^{1)*}, E. Dewald¹⁾, K. Campbell^{1)†}, R. Turner¹⁾, F. Weber¹⁾, M. Rhodes¹⁾, O. Landen¹⁾, M. B. Schneider¹⁾, D. Lee¹⁾, V. Tran²⁾, D. Pellinen²⁾

¹⁾ *Lawrence Livermore National Laboratory, P.O. Box 808, Livermore CA, 94550, USA*

²⁾ *Bechtel Nevada, Livermore Operations, Livermore, CA, USA*

**E-mail: schein2@llnl.gov*

Radiation drive diagnostics during the NIF early light campaign was supported by an 18 channel soft x-ray spectrometer (Dante). In order to achieve a measurement accuracy of 2% in radiation temperature absolute calibration of the individual channels was necessary and signal distortion through long transmission lines had to be compensated for as well. For fast signals the signal attenuation due to the long (50m) cables amounted to ~20%@100MHz, which was corrected by a cable compensation in the frequency domain. The varying effects of cable distortion for a variety of signals between 1ns and 9ns in length were evaluated and corrections were applied.

Results of the thus calculated temperatures of the NEL campaign will be presented compared to LASNEX predictions, showing agreement in peak radiation temperature within less than 2%.

[†]now with Acree Technologies, Concord, CA

Introduction

During the NIF early light (NEL) campaign in 2004 the Dante soft x-ray power diagnostics^{1,2} was commissioned to measure the energetics inside a half hohlraum driven by a single quad with a maximum energy of 17kJ for pulse lengths ranging from 1ns to 9ns^{3,4}. The resulting soft x-ray flux produced inside the half hohlraums is detected using 18 absolutely calibrated channels consisting of filters, detectors and, for the soft channels, grazing incidence mirrors, each one covering a distinct spectral range from 50eV to 20keV². The signals produced by each of the 18 channels are used to modify a Black Body spectrum, thus resulting in an energy dependent x-ray flux distribution. Integration over the spectral flux distribution is subsequently used to define a radiation temperature $T_{RAD}=(\Phi/\sigma A)^{0.25}$, which is compared to results of simulations produced by LASNEX.

Signal production and transmission

During the NEL campaign the obtained peak T_{RAD} are shown to have reached values up to ~330eV ($\Phi \sim 10^5$ GW/sr) using small half-hohlraums and 1.1ns laser pulses⁵. These fluxes produce signals of up to 50V in the x-ray detectors, with a rise time of ~100ps. The signals are transmitted through 50m long Times Microwave LMR 600 cables, with a nominal loss of 4.43dB/33m at 2.4Ghz⁶. After appropriate attenuation using PSPL attenuators the signals are directed through a 50:50 splitter, where an additional fiducial signal is added to cross-time the individual channels, into transient waveform digitizers Tektronix SCD5000 with an analog bandwidth of ~4.5GHz. A schematic describing the signal flow is shown in figure 1. All electronic parts used are calibrated using network analyzers over a frequency range from DC to 10GHz, with the exception of the signal

cable, which are tested using defined fast rising voltage pulses. Due to the limited frequency response of the electronic parts in the signal path the transmitted signal becomes increasingly distorted with increasing signal frequency. Further ohmic losses in the system produce additional signal attenuation independently of the frequency.

While attenuators and splitter have been demonstrated to transmit signals without any significant distortion up to 5 GHz, the length of the cable causes measurable attenuation even at frequencies as low as 10MHz, which can be demonstrated looking at the signal distortion of a 10ns square pulse produced by a PPL 10050 pulse generator with a 45ps rise time (figure 2). The cable attenuates the signal as much as 10% at 10MHz increasing to ~50% at 1GHz. The measured attenuation using the test pulses can be compared to the nominal attenuation from⁶, as shown in figure 3. At 5 GHz the measured attenuation is 80%, whereas the nominal value amounted to 70%. These deviations can be explained by the use of connectors and small variations in cable length.

Signal restoration

A compensation for the measured cable losses has to be implemented in order to restore the signal generated by the x-ray detectors before going through the cable $x(t)$. The distortion can be described as a result of the convolution of the input signal $x(t)$ with the cable response $h(t)$ resulting in the output signal measured in the digitizers $y(t)$:

$$y(t)=x(t)*h(t).$$

As the deconvolution in the time domain is fairly complex we have applied a cable loss compensation in the frequency domain, which results in a simple multiplication if the transfer function $H(f)=F(h(t))$ (F denotes Fourier transform) is known. To obtain the

transfer function $H(f)$, the cable is tested with a well known signals $x'(t)$ to obtain $y'(t)$, which allows us to define: $H(f)=F(y'(t))/F(x'(t))$

Using this approach is limited by the choice of $x'(t)$. While an ideal delta function would be most suitable due to the flat frequency of its Fourier transform, the actual production of such a signal with pulse generators is impossible. Using the derivative of a fast rising pulse to obtain such a delta pulse would require additional lengthy software code to ensure the correct position in time and the offset/DC compensation as using a derivative would eliminate these components.

For the NIF Dante a square pulse has been chosen, with a fast rising and a fast falling edge, which realized by a conventional pulser PSPL 10050. This method can be problematic as an ideal 10ns pulse creates zero values in the Fourier transform at multiples of 100MHz, which has to be taken into account. However, with expected signals being much faster than 100MHz this should not produce any issues. Thus once the test signal is obtained $H(f)$ can be created, and used to restore the original signals applying:

$X(f)=Y(f)R(f)/H(f)$, where $R(f)$ is a data dependent filter function used to reduce the noise produced by the Fast Fourier Transform, first described by Nahman⁷.

$$R(f)=|H(f)|^2/(|H(f)|^2+\gamma|C(f)|^2)$$

$$C(f)=\sin^4(2\pi f/F)$$

$$R(f)/H(f)=H^*(f)/(|H(f)|^2+\gamma|C(f)|^2)$$

To validate this approach a blind test has been used employing a shaped pulse transmitted through a signal cable. Figure 4 shows a summary of the original pulse, the

distorted pulse and the result of the compensation performed as described above. The maximum error observed for this experiment was 2%.

After this verification the cable compensation is used for the NEL experiments. Examples of channel responses for a 2ns pulse, showing real data, are presented in figure 5, demonstrating the significant distortion of the Dante signals by the cable for a mirrored and non-mirrored channel.

Data analysis

After restoring the signals of each of the 18 channels and taking into account the influence of attenuators and splitters the signals are lined up in time using fiducial signals, which have been calibrated in time with respect to the 5% rise of a fast test pulse. Hence it is possible to correct for the different travel times of the x-rays from target chamber center to the individual detectors and the slight variations in cable length of each channel. Delay times of additional parts like attenuators are measured individually and used for correction as well.

Once the correct signals have been assembled the flux in individual energy bands, defined by the response functions², is calculated using the measured signals from each channel with a step size of 100ps, taking also into account the solid angle for each channel defined by apertures in the Dante system. This method produces energy spectra at each step in time, allowing for spectral analysis of the soft x-radiation. Integrating over the thus obtained flux distribution results in total flux vs time plots for each experiment. The flux is then converted to a radiation temperature using the effective source size.

Error analysis

The error in the analysis of the Dante signal is compounded from various sources. Aside from the cable compensation, which has been shown to produce up to 2% in flux the largest contributor is the calibration of the individual channels. With decreasing filter thickness (i.e. lower energy) calibration becomes increasingly inaccurate. Calibration errors can amount to as much as 10% close to absorption edges at lower energies. In addition, with decreasing radiation temperature the number of channels producing usable signals is reduced, which increases the error of the total flux calculation. Figure 6a shows the dependency of signal strength in the individual channels as function of radiation temperature. As a result of this the flux error due to calibration ranges from $\pm 1.5\%$ at 300 eV to nearly $\pm 4\%$ at 80eV as shown in Figure 6b. Other errors include measurement tolerances in the calibration of attenuators and splitters, which amount to an additional 2% in flux in the case of three attenuators in series, which fortunately are used only in case of high radiation temperatures, where the effect of the calibration error is reduced. Apart from these instrumentation errors the Dante analysis is influenced by experimental tolerances. The biggest source of error is in the source size, i.e. in case of hohlraums diagnostic hole or Laser Entrance Hole. Any error in source size will translate into an error in radiation temperature of $(\Delta x)^{0.25}$. Assuming an uncertainty of 5% will translate into a flux error of 1.3%. Thus the assumption can be made that the radiation flux can be determined within $\sim 6\%$ for hot Hohlraums to $\sim 8\%$ for cold Hohlraum resulting into a radiation temperature error from 2% (300eV) to 3% (80eV).

Results

The results of the Dante analysis are presented here by looking at a series of experiments using 2 ns flat-top pulses and variable laser energy in the 5-13 kJ range, which allowed us

to measure the radiation temperature scaling with laser power and hohlraum size under conditions where minimal plasma filling was expected and thus a constant source size can be assumed. We used cylindrical Au hohlraums of various sizes with a single LEH and irradiated the hohlraum back wall with the four laser beams effectively forming an $f/8$ cone that propagates along the hohlraum axis. Dante has a partial view of the initial laser spots on the hohlraum back wall and provides a measure of the radiation flux that includes both the primary laser-plasma emission and the re-emitting walls. Figure 7 shows the results of the measurements for cable compensated and raw data and figure 8 compares measured/cable compensated and predicted radiation temperatures for scale-1 (1.6 mm diameter, 1.5 mm long) and scale-3/4 (1.2 mm diameter, 1.1 mm long) hohlraums with a LEH size of 0.75 of the hohlraum diameter as well as the Dante view of the target and laser spots². We find that the radiation temperature scales as expected with both the laser power and hohlraum size from detailed LASNEX simulations⁸ and from analytical scaling laws⁹. The peak radiation temperature between Dante data and LASNEX calculations agree within the experimental Dante radiation temperature error bar of $\sim 2\%$.

In addition to the 2ns pulse experiments we performed long pulse (6ns, 9ns) experiments using larger, scale-3/2 hohlraums and scale 3/8 hohlraums driven by a 1.1 ns pulse⁵.

Figure 9 shows a summary of the radiation temperature through the LEH T_{LEH} for all experiments as measured by Dante, and simulated by LASNEX. As can be seen from the data the peak radiation temperature measured by Dante fits the simulation for all cases. The overall agreement seems to improve for longer pulses, hinting at an undercompensation in the beginning of the pulse (i.e. for higher frequencies).

Conclusion:

The Dante soft x-ray spectrometer for the NIF is a high resolution tool for soft x-ray analysis. Corrections applied for signal attenuation due to the frequency response of the electrical system can amount to $> 50\%$ for signals faster than 1GHz. In the realm of the described experiments signal correction near the peak of the flux were of the order 10%. It has been shown that a compensation for the system attenuation can be applied with a residual error of 2% in the peak, even though a larger error early in the pulse is observed, which might be due to uncompensated losses in other parts of the transmission path, which will have to be addressed in future experiments. The system has been shown to measure the soft x-ray flux to $\sim 8\%$, which corresponds to a radiation temperature uncertainty of $\sim 2\%$. Results of measurement taken by Dante agreed with LASNEX calculations in the peak to within the calculated error bars.

Acknowledgements

The authors acknowledge the valuable input of J. Blair of Bechtel Nevada, and S. Vernon of LLNL.

This work was performed under the auspices of the U.S. Department of Energy by the Lawrence Livermore National Laboratory under contract W-7409-Eng-48.

References

- [1] H.N. Kornblum, R.L. Kauffmann and J.A. Smith, Rev. Sci. Instrum. **57**, 2179 (1986)
- [2] E.L. Dewald et al., Rev. Sci. Instrum. **75**, 3759 (2004).
- [3] E.L. Dewald et al., Phys. Rev. Let. **95**, 21 (2005)

Jochen Schein 5/1/06 3:01 PM
Formatted: English (US)

[4] E.L. Dewald et al. PoP

[5] D. Hinkel et al., Phys. Plasmas, **12**, 056305 (2005).

[6] <http://www.ocarc.ca/coax.htm>

[7] Nahman TBS Tech Note

[8] G.B. Zimmerman, W.L. Kruer, Comm. Plasma Phys. Contr. Fusion **2**, 51 (1975).

[9] R. Sigel et al., Phys. Rev. Lett. **65**, 587 (1990).

Jochen Schein 5/1/06 3:30 PM

Formatted: French

Jochen Schein 5/1/06 3:30 PM

Formatted: French

Jochen Schein 5/1/06 3:01 PM

Formatted: German

Jochen Schein 5/1/06 3:01 PM

Formatted: English (US)

Figure captions

Figure 1: Signal flow in the Dante diagnostics system

Figure 2: Input signal and transmitted output signal showing signal attenuation by a 50m long LMR 600 cable

Figure 3: Nominal and measured attenuation caused by 50m LMR 600 cable

Figure 4: Original pulse (dotted), distorted (solid) pulse and restored (dashed) pulse using deconvolution in frequency domain

Jochen Schein 5/1/06 3:35 PM

Deleted: solid

Figure 5: Distorted (solid) signal and reconstructed (dashed) signal for 2ns 5kJ laser drive pulses. Right: Channel 1 (50-70eV) response, Left: Channel 6 (900-980eV)

Figure 6: a) Signals produced in 18 channels, positioned at the mean channel energy for different radiation temperatures including the noise level of the system. b) Flux and Trad error as a function of radiation temperature due to calibration uncertainties

Figure 7: Effect of cable compensation on Dante flux measurement result for 2ns, 5kJ laser pulse driven scale 1 hohlraum

Figure 8: Summary of radiation temperature through the LEH T_{LEH} for 2 ns driven hohlraum as measured by Dante, and simulated by LASNEX

Figure 9: Summary of radiation temperature through the LEH T_{LEH} for all experiments showing the dynamic range of Dante, and simulated by LASNEX

Figures:

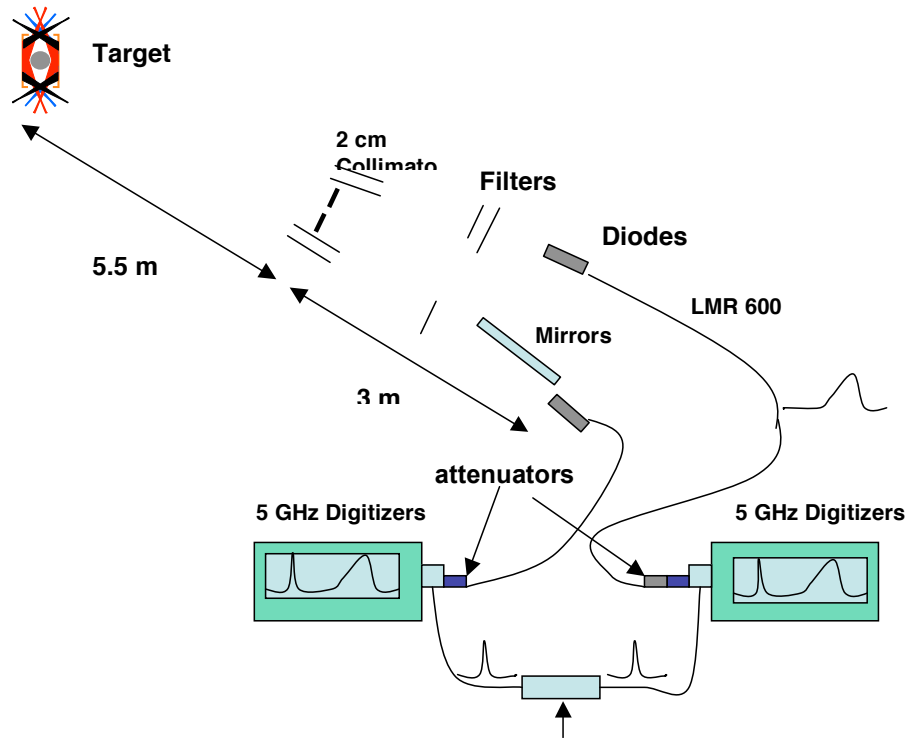


Figure 1:

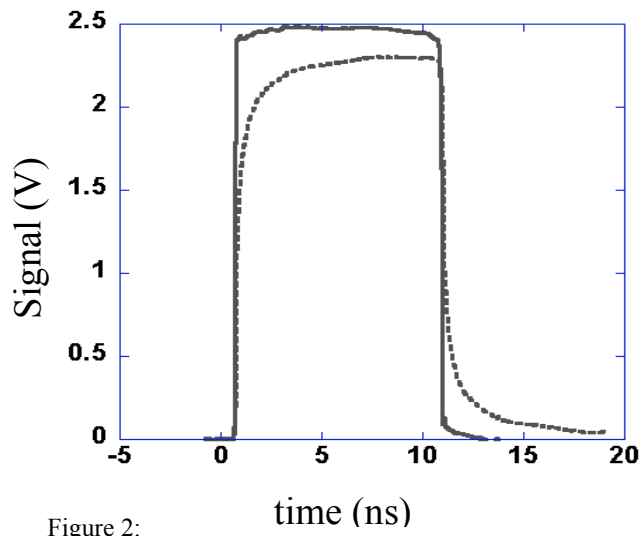


Figure 2:

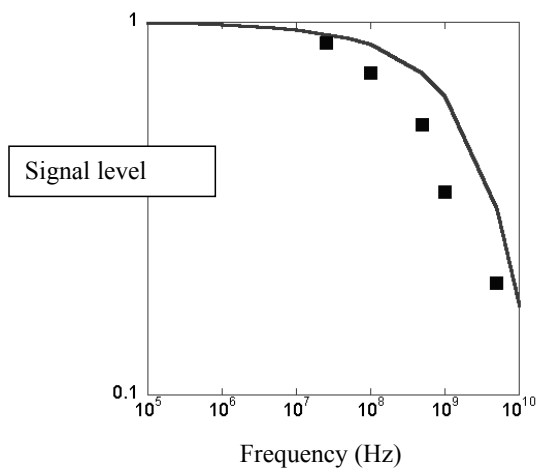


Figure 3:

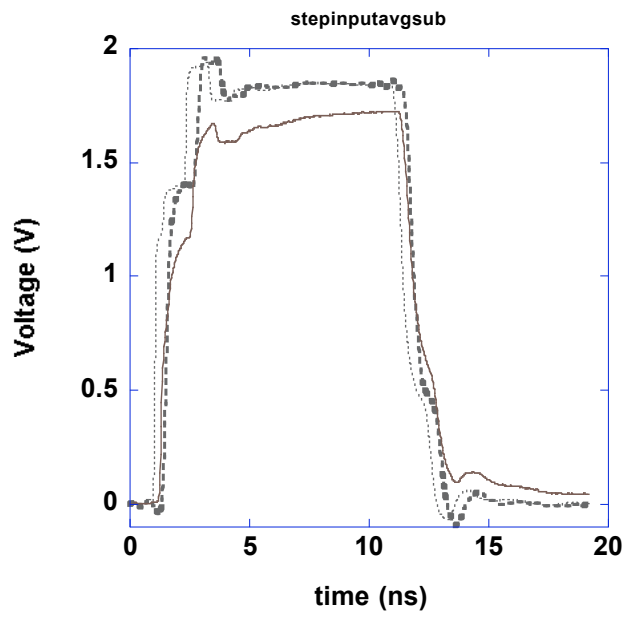


Figure 4:

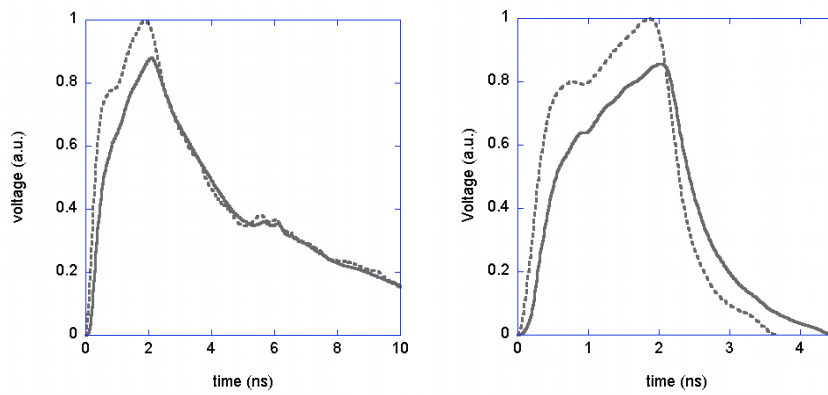


Figure 5:

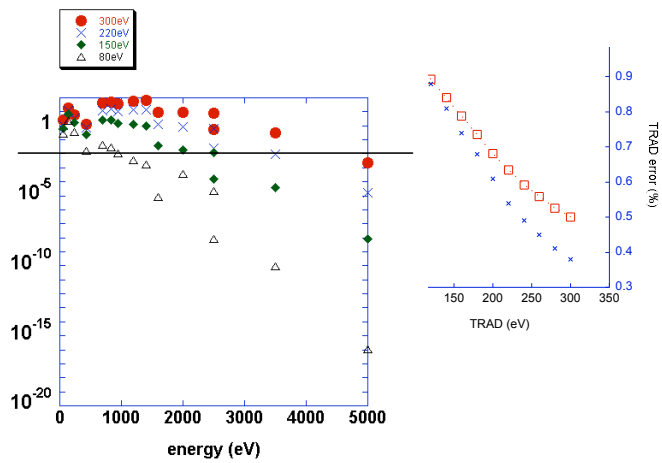


Figure 6a left, 6b right:

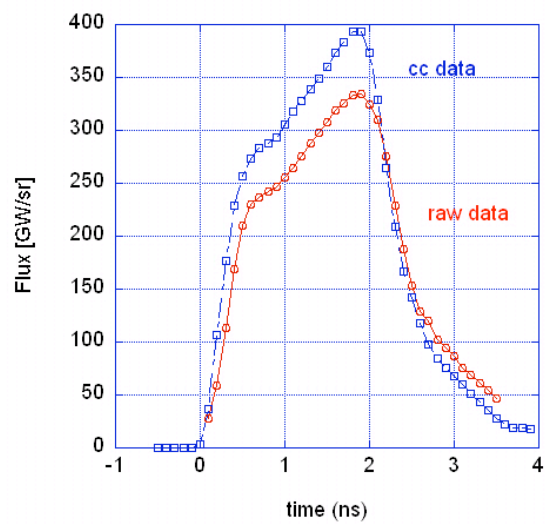


Figure 7

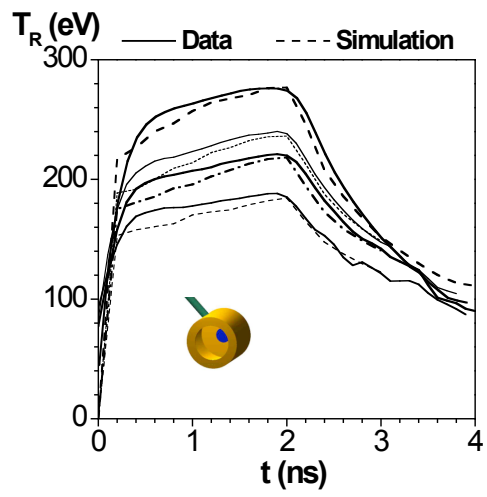


Figure 8:

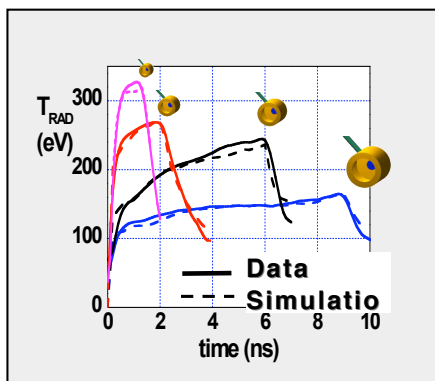


Figure 9: